Journal of Theoretical Biology 421 (2017) 28–38

Contents lists available at ScienceDirect

Journal of Theoretical Biology

journal homepage: www.elsevier.com/locate/jtbi

Effects of rainfall on *Culex* mosquito population dynamics

L.D. Valdez[a,b,*], G.J. Sibona[a,b], L.A. Diaz[c,d], M.S. Contigiani[d], C.A. Condat[a,b]

[a] Facultad de Matemática, Astronomía, Física y Computación, Universidad Nacional de Córdoba
[b] Instituto de Física Enrique Gaviola, CONICET, Ciudad Universitaria, 5000 Córdoba, Argentina
[c] Instituto de Investigaciones Biológicas y Tecnológicas–CONICET–Universidad Nacional de Córdoba, Córdoba, Argentina
[d] Laboratorio de Arbovirus–Instituto de Virología "Dr. J. M. Vanella"–Facultad de Ciencias Médicas–Universidad Nacional de Córdoba, Córdoba, Argentina

ARTICLE INFO

Article history:
Received 25 October 2016
Revised 22 February 2017
Accepted 25 March 2017
Available online 27 March 2017

Keywords:
Culex
Rainfall
Arbovirus
Mosquito abundance
Mathematical modeling

ABSTRACT

The dynamics of a mosquito population depends heavily on climatic variables such as temperature and precipitation. Since climate change models predict that global warming will impact on the frequency and intensity of rainfall, it is important to understand how these variables affect the mosquito populations. We present a model of the dynamics of a *Culex quinquefasciatus* mosquito population that incorporates the effect of rainfall and use it to study the influence of the number of rainy days and the mean monthly precipitation on the maximum yearly abundance of mosquitoes M_{max}. Additionally, using a fracturing process, we investigate the influence of the variability in daily rainfall on M_{max}. We find that, given a constant value of monthly precipitation, there is an optimum number of rainy days for which M_{max} is a maximum. On the other hand, we show that increasing daily rainfall variability reduces the dependence of M_{max} on the number of rainy days, leading also to a higher abundance of mosquitoes for the case of low mean monthly precipitation. Finally, we explore the effect of the rainfall in the months preceding the wettest season, and we obtain that a regimen with high precipitations throughout the year and a higher variability tends to advance slightly the time at which the peak mosquito abundance occurs, but could significantly change the total mosquito abundance in a year.

1. Introduction

Mosquito-transmitted flaviviruses are an increasing health threat. In particular, members of *Culex* species (Diptera: Culicidae) such as *Cx. quinquefasciatus* and *Cx. interfor* are responsible for transmitting the West Nile and St. Louis encephalitis (SLEV) viruses to humans and domestic animals (Beltrán et al., 2015; Diaz et al., 2008; 2016; Gubler, 2002; Gubler et al., 2007; Lumsden, 1958). For instance, the SLEV is endemic in Argentina, where the principal vector is postulated to be *Cx. quinquefasciatus* (Diaz et al., 2013). In the last decades, mosquito-borne diseases have emerged and re-emerged as a result of multiple factors such as increasing urbanization, international travel, and climate change (Harrigan et al., 2014; Kilpatrick, 2011). The development of mathematical models is essential to quantify the effect of each of these factors on the dynamics of the mosquito population, and to determine the most effective strategies to control the epidemic outbreaks transmitted by mosquito vectors (Anderson et al., 1992; Ewing et al., 2016; Lord and Day, 2001a; 2001b; Marini et al., 2016).

Multiple studies have shown that the life cycle of the *Cx. quinquefasciatus* is closely related to temperature (Almirón and Brewer, 1996; Ciota et al., 2014; Gunay et al., 2011; Loetti et al., 2011; Strickman, 1988). Strickman (1988) demonstrated that its reproductive activity increases with temperature, and Almirón and Brewer (1996) showed that this species can only live in environments with a temperature above 10 °C. Other studies have found that temperature has a strong influence on the development and survival of both adult and immature mosquitoes (Ciota et al., 2014; Gunay et al., 2011; Loetti et al., 2011). In turn, it was observed that *Cx. quinquefasciatus* does not enter diapause, but it may undergo quiescence or remain gonoactive in protected (indoor or underground) habitats (Almirón and Brewer, 1996; Nelms et al., 2013). Urbanization therefore helps *quinquefasciatus* populations survive the mild winters of temperate regions.

Similarly, rainfall is an important climatological variable to predict the abundance of *Culex* mosquitoes, since its copiousness and distribution determine the production and size of mosquito breeding sites. Reisen et al. (2008) studied the changes in the *Cx. tarsalis* population in California and found that, in most regions, it is positively correlated with an increase in total precipitation. However, these authors also found that in some places of the driest region of California, the correlation between these two variables was neg-

* Corresponding author.
E-mail address: lvaldez@famaf.unc.edu.ar (L.D. Valdez).

http://dx.doi.org/10.1016/j.jtbi.2017.03.024
0022-5193/

ative. On the other hand, Olson et al. (1983) showed that a very large rainfall is not always accompanied by proportionately large increases in the abundance of *Cx. tritaeniorhynchus* and *Cx. gelidus*. In consequence, these results indicate that there exists a nonlinear relationship between rainfall and *Culex* abundance, which should be modeled in order to predict mosquito abundance. Additionally, since the climatological projections suggest that global warming will alter the frequency and intensity of rainfall, it is crucial to understand how different rainfall patterns will affect mosquito populations.

In this paper we develop a dynamic model of the *Cx. quinquefasciatus* population, adapting a fracturing procedure (Finley and Kilkki, 2014) to describe the rainfall distribution. We use a system of compartmental ordinary differential equations that describe the immature and adult mosquito populations, in which we introduce the influence of temperature and rainfall on the reproduction rate. To study the influence of different rainfall patterns, we use a synthetic time series of rainfall based on the amount of rainfall per month and the monthly number of rainy days. We find that, for a given constant value of monthly precipitation, there is an optimum number of rainy days for which the maximum M_{max} in the mosquito population is highest.

On the other hand, we also study the variability of daily rainfall intensity through a fracturing process (Finley and Kilkki, 2014), which allows us to study homogeneous and heterogeneous rainfall regimes, including those characterized by heavy rain events. We show that increasing daily rainfall variability reduces the dependence of M_{max} on the number of rainy days, leading also to a higher abundance of mosquitoes for the case of low mean monthly precipitation.

Finally, we explore the effect of different winter precipitation regimes on the mosquito abundance in the summer season, obtaining that a higher variability tends to advance slightly the peak time of mosquito abundance. Interestingly, we predict that the accumulated abundance of mosquitoes will decrease in a regime with high variability in the rainfall intensity.

The boundary of the *Cx. quinquefasciatus* habitat in South America runs across central Argentina. This region is thus expected to exhibit intense changes in mosquito populations due to the undergoing climatic change; this is likely to have a strong impact on flavivirus prevalence. For this reason, we use the climatic data for the city of Córdoba to calibrate our model in the period 2008–2009.

The paper is organized as follows: in Section 2.1 we present the model of the dynamics of mosquito population and in Section 2.2 and 2.3 we explain the methods for generating two different synthetic time series of rainfall. Then in Section 3 we show our results and finally we present our conclusions in Section 4.

2. Methods

2.1. The model of mosquito abundance

In this section, we construct a compartmental, ordinary differential equation model for the mosquito abundance. We consider that the total vector population is stage-structured with an immature class consisting of all aquatic stages, and a mature or adult class . We assume that these population groups are restricted only to female mosquitoes as the reproductive sex.

In our model, the total birth rate, *i.e.* the total number of new immature female mosquitoes per unit of time, is proportional to the number of adult mosquito females and to $\beta_L\lambda(t)\theta(t)$, where β_L corresponds to the reproduction rate in optimal conditions of temperature and water availability, and $\lambda(t)$ and $\theta(t)$ are normalized factors describing the influence of rainfall and temperature on the total birth rate, respectively. In Section 2.1.1 we will explain how we construct these factors. In addition, we assume that the total birth rate is also regulated by a carrying capacity effect that depends on the occupation of the available immature habitats. Therefore we propose that the immature population growth is logistic-like with a carrying capacity K_L. Additionally, immature individuals either go to the mature class with rate m_L or die at a rate μ_L. We stress that the ratio $1/m_L$ gives the average development time from immature mosquito to adult. Finally, adult mosquitoes die with a mortality rate μ_M. For simplicity, we assume that m_L, μ_L and μ_M do not depend on temperature or rainfall. With these definitions, we propose the following dynamic mass-balance equations for the abundance of immature mosquitoes, $L(t)$, and adult mosquitoes, $M(t)$,

$$L(t+\Delta t) = L(t) + \Delta t\left[\beta_L\theta(t)\lambda(t)M(t)\left(1-\frac{L(t)}{K_L}\right) - m_L L(t) - \mu_L L(t)\right], \tag{1}$$

and

$$M(t+\Delta t) = M(t) + \Delta t[m_L L(t) - \mu_M M(t)], \tag{2}$$

where Δt is the time step size. Here we use $\Delta t = 0.1$ [days]. Eq. (1) can be easily derived by assuming that the fraction of the carrying capacity corresponding to female immature mosquitoes is the same as the fraction of females in the immature population. Table 1 summarizes the different state variables and parameters used in this paper.

2.1.1. Effect of temperature and rainfall on the total birth rate

We add the effect of the temperature through a temperature factor $\theta(t)$. Several studies have shown that *Cx. quinquefasciatus* can breed only at temperatures above 10 °C (Almirón and Brewer, 1996; Ribeiro et al., 2004) and that the number of egg rafts collected per day is closely correlated with temperature (Strickman, 1988). Therefore we propose that the factor $\theta(t)$ is a piecewise linear function,

$$\theta(t) = \begin{cases} \dfrac{T(t)-T_A}{T_B-T_A} & \text{if} \quad T_A \leqslant T(t) \leqslant T_B \\ 1 & \text{if} \quad T(t) > T_B \\ 0 & \text{if} \quad T(t) < T_A, \end{cases} \tag{3}$$

where $T(t)$ is the average daily temperature and $T_A = 10$ °C corresponds to a minimum temperature below which the net birth rate vanishes. The choice of the function $\theta(t)$ is not unique: for instance, a power law may be used instead (Ewing et al., 2016). Here we assume that the positive effect of the temperature on the birth rate saturates at T_B, since it was observed by Oda et al. (1980) that the number of egg raft per female does not significantly change between 21 °C and 30 °C.

On the other hand, mosquito reproduction is also triggered by rainfalls since these increase the number of breeding sites, such as temporary ground pools. In order to introduce the effect of rainfall on the mosquito birth rate, we compute the accumulated amount of rainwater H, whose variation is given by the total daily rainfall $R(t)$ minus the evapotranspiration $E(t)$ (Gong et al., 2011),

$$H(t+1) = H(t) + [R(t) - E(t)]. \tag{4}$$

The function $H(t)$ is a convenient measure of the quantity of water available for breeding sites. It should represent the average level of puddles, ponds, drains, small streams, and underground sources such as waste water channels in urban environments. As we will explain below, Eq. (4) is applied on a daily time scale. The term of evapotranspiration is estimated using the Ivanov model (Romanenko, 1961; Valipour, 2014) which is based on the mean temperature and the relative humidity [$Hum(t)$], and it is given by

$$E(t) = 6.10^{-5}(25 + T(t))^2(100 - Hum(t)). \tag{5}$$

Table 1
The variables and parameters for Eqs. (1)–(9).

Quantity	Definition	Value	Refs.
L	Number of immature female mosquitoes	–	
M	Number of adult female mosquitoes	–	
β_L	Birth rate of immature female mosquito per female adult mosquito in optimal conditions of temperature and water availability (1/days^{-1})	13.5	fitted (see Appendix A)
θ	Effect of the temperature on the birth rate of mosquitoes	–	
λ	Effect of the water availability on the birth rate of mosquitoes	–	
m_L	Rate at which immature mosquitoes develop into adults (1/days^{-1})	0.098	Loetti et al. (2011)
μ_L	Immature mortality rate (1/days^{-1})	0.03	Loetti et al. (2011)
μ_M	Mosquito mortality rate (1/days^{-1})	0.078	David et al. (2012)
K_L	Carrying capacity of the immature female population	16.2	fitted (see Appendix A)
H_{max}	Maximum daily amount of accumulated rainwater [mm]	9.86	fitted (see Appendix A)
H_{min}	Minimum daily amount of accumulated rainwater [mm]	0.067	fitted (see Appendix A)
H	Accumulated amount of rainwater [mm]	–	
R	Daily rainfall [mm]	–	
E	Daily evapotranspiration [mm]	–	
T	Average daily temperature [°C]	–	
Hum	Daily relative humidity	–	
P_{max}	Total rainfall in the wettest month [mm]	–	
P_{min}	Total rainfall in the driest month [mm]	–	
D_{max}	Total number of rainy days in the wettest month [days]	–	
D_{min}	Total number of rainy days in the driest month [days]	–	

Note that the evapotranspiration $E(t)$ is a monotonically increasing function of temperature and a decreasing function of humidity. In particular, $E(t)$ vanishes for $Hum = 100\%$. In addition, we assume that the level of accumulated water H varies only between a minimum (H_{min}) and a maximum (H_{max}) boundary level, *i.e.*,

$$H(t+1) = \begin{cases} H_{\min} & \text{if } H(t)+R(t)-E(t) \le H_{\min} \\ H_{\max} & \text{if } H(t)+R(t)-E(t) \ge H_{\max} \\ H(t)+R(t)-E(t) & \text{otherwise.} \end{cases} \quad (6)$$

Here, H_{min} represents a minimum amount of water that is always available for mosquito breeding, for instance in permanent streams or in the drainage system, while H_{max} is a level of water above which the breeding sites overflow (Karl et al., 2014).

Finally, the factor $\lambda(t)$ that takes into account the effect of rainfall on the birth rate (see Eq. (1)), is the normalization of $H(t)$:

$$\lambda(t) = \frac{H(t)}{H_{max}}. \quad (7)$$

Note that the minimum value of $\lambda(t)$ is H_{min}/H_{max}.

Although we take the integration time step to be $\Delta t = 0.1$ days, the data of temperature, rainfall and humidity are available only on a daily time scale. Therefore, for all the integration time steps within a day "d" (i.e. $d \le t < d+1$), we set $\lambda(t)$ and $\theta(t)$ to have the values computed through Eqs. (6) and (5) using the corresponding meteorological data at day "d".

2.2. Model of synthetic rainfall using the monthly number of rainy days and the monthly precipitation

The amount of average rainfall P and the number of days D with rain per month are two parameters commonly used to characterize the long-term precipitation trend (Madsen et al., 2009; Owusu and Waylen, 2013; Zhai et al., 2005). In this section, we show how they can be used to construct a synthetic rainfall time series.

The average monthly rainfall is assumed to follow a sinusoidal function,

$$P(m) = \frac{P_{max}-P_{min}}{2}\cos\left(\frac{2\pi}{12}(m-m_0)\right) + \frac{P_{max}+P_{min}}{2}, \quad (8)$$

where $m = 1, \ldots, 12$ represents the month (with $m = 1$ for January and $m = 12$ for December), m_0 corresponds to the month of maximum rainfall, P_{max} is the total precipitation of the wettest month m_0, and P_{min} is the total precipitation of the driest month, corresponding to $m = m_0 + 6$. Note that for a higher value of either P_{max} or P_{min} there is an increase in the annual amount of precipitation but, while a higher P_{max} enhances the precipitation difference between the rainy and dry seasons, a higher P_{min} reduces this difference.

Similarly, we propose that the number of rainy days is given by

$$D(m) = \frac{D_{max}-D_{min}}{2}\cos\left(\frac{2\pi}{12}(m-m_0)\right) + \frac{D_{max}+D_{min}}{2}, \quad (9)$$

where D_{max} and D_{min} correspond to the number of rainy days in the months labeled by m_0 and $m_0 + 6$, respectively. Choosing $m_0 = 2$, this distribution would be suitable for the city of Córdoba. In Fig. 1(a) and (b) we show a schematic of the parameters used in Eqs. (8) and (9).

From Eqs. (8) and (9) we construct the amount of daily rainfall $R(t)$ (see Eq. (4)), placing the rainy days in each month at random and assuming that the amount of rain specified in Eq. (8) is equally distributed over these days. Then we calculate the factor $\lambda(t)$ and integrate Eqs. (1) and (2). For simplicity we use in these equations the values of humidity and temperature obtained from meteorological data.

It is important to note that, by construction, $R(t)$ is a stochastic time series since the rainy days for each month are chosen at random; therefore our results for the effect of the synthetic series $R(t)$ on the mosquito abundance must be averaged over a large number (we take 10^4) of realizations. Using this model of time series of rainfall, we measure the highest peak of mosquito abundance M_{max} and the time τ_{max} at which this peak is reached (see Fig. 1(c)).

In the following section, we explain how to introduce variability on the amount of daily rainfalls.

2.3. Model of synthetic rainfalls with variable daily intensity of precipitation

In general, the daily rainfall intensity can range from drizzles with less than 1 mm to torrential downpours exceeding

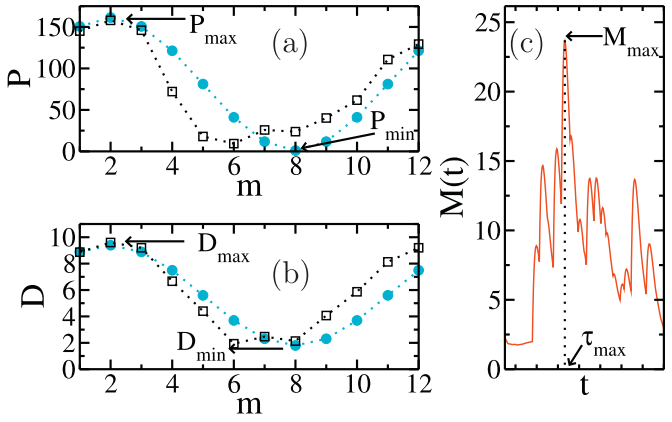

Fig. 1. Schematic representation of Eq. (8) (panel (a)) and Eq. (9) (panel (b)), where $P(m)$ is the monthly amount of rainfall and $D(m)$ is the number of rainy days per month (blue circles). In these plots we also show the average monthly precipitation and number of rainy days in the city of Córdoba in the period 2001–2015 (black squares) (Wunderground (2016)). Panel (c) is a cartoon of $M(t)$ indicating the maximum abundance of mosquitoes M_{max} and the time τ_{max} (in day units) at which this peak is reached. Dotted lines are to guide the eye. (For interpretation of the references to color in this figure legend, the reader is referred to the web version of this article.)

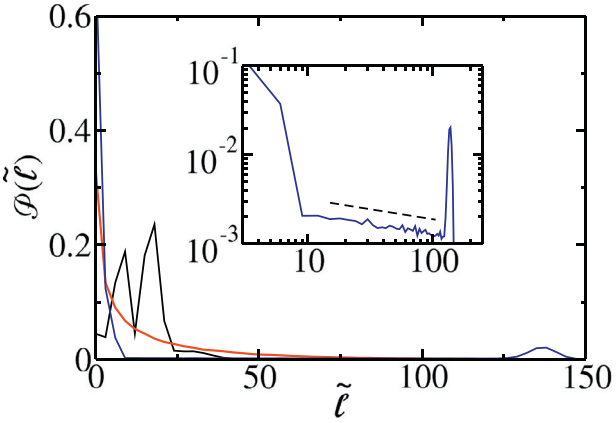

Fig. 2. Distribution of length segments $\mathcal{P}(\tilde{\ell})$, using $\ell = 150$ mm (total length) and $D = 10$ (number of rainy days) for different values of α: 0.1 (black), 0.5 (red), and 0.9 (blue). These distributions were obtained over 2.10^4 realizations. In the inset, we show $\mathcal{P}(\tilde{\ell})$ for $\alpha = 0.9$ in log-log scale, and the dashed line corresponds to a power-law fit with an exponent 0.22. (For interpretation of the references to color in this figure legend, the reader is referred to the web version of this article.)

200 mm (Lei et al., 2008; Li et al., 2013). Various distributions, such as Weibull (Suhaila and Jemain, 2007), lognormal (Cho et al., 2004) and generalized Pareto (Deidda, 2010), have been proposed to model the precipitation amount. While the above-mentioned distributions could be used to generate a sequence of rainfalls with variable or heterogeneous intensity, the disadvantage of this approach is that the total monthly rainfall is also a stochastic variable. In order to isolate the effect of the heterogeneity of the rainfalls, we will use a fracturing or fragmentation process (FT), which allows us to maintain the total monthly rainfall constant. This method is related to a cascading procedure that was used by physicists to study the fragmentation of brittle material (Hernandez, 2003). Recently the FT process was also applied to obtain empirical distributions with a finite tail (Finley and Kilkki, 2014). From a geometrical point of view (Borgos, 2000; Finley and Kilkki, 2014), this process performs a sequential breakage of a segment or interval of length ℓ to obtain D subintervals with variable length $\tilde{\ell}$, which can be used to decompose the total monthly rainfall into daily rainfalls with heterogeneous intensity. In this representation, ℓ and $\tilde{\ell}$ stand for the total amount of rainfall in a month and in a day, respectively. In Appendix B we explain the steps of the FT process in detail.

This method depends on a parameter $\alpha \in [0, 1]$ which controls the heterogeneity of the segment length. In particular:

- $\alpha = 0$ corresponds to the case where an interval is split into two subintervals of equal length $\tilde{\ell} = \ell/2$,
- $\alpha = 1$ corresponds to the special case where two "intervals" are generated, one of length zero and the other of length $\tilde{\ell} = \ell$.

In Fig. 2 we show how α controls the shape of the fragment length distribution $\mathcal{P}(\tilde{\ell})$, using $\ell = 150$ mm and $D = 10$. Note that the resulting length of each subinterval corresponds to the intensity of rainfall in one day.

For small values of α the distribution is concentrated around the mean value close to ℓ/D, while for intermediate values of α, the distribution of lengths has a longer tail. Finally, for high values of α, $\mathcal{P}(\tilde{\ell})$ has a peak near ℓ which depicts a regime where most of the corresponding month total rainfall is confined to one day. Interestingly, we also note that in this case the rainfall distribution has a region in which it decays as a power law.

In order to model the temporal variation of precipitation $R(t)$ (see Section 2.1.1), we apply a fracturing process (FT) for each month, partitioning an interval whose length is the amount of monthly precipitation given by Eq. (8) and where the number of subintervals (the number of rainy days) is given by Eq. (9). See Appendix B for further details on the construction of $R(t)$.

3. Results

3.1. Calibration

We calibrate our model of mosquito abundance using a Metropolis-Hastings algorithm (see Appendix A) with the number of female *Culex quinquefasciatus* mosquitoes collected in Córdoba city (31°24′30″ S, 64°11′02″ W, Córdoba province, Argentina) every two weeks from January 2008 to December 2009 (see Batallán, 2013; Batallán et al., 2015 for details on the data and their sources). The climate of Córdoba is temperate with dry winters and hot rainy summers. The mean annual temperature ranges between 16 °C and 17 °C and the mean annual rainfall is 800 mm (Jarsún et al., 2003). The temperature $[T(t)]$, relative humidity $[Hum(t)]$, and rainfall $[R(t)]$ data for Córdoba were obtained from the website (Wunderground, 2016). We calibrate the following parameters: β_L, H_{max}, H_{min}, and K_L. In Appendix C we perform a sensitivity analysis of these calibrated parameters.

As initial conditions of Eqs. (1) and (2), we set $M(t) = L(t) = 20$. To attenuate the effect of these initial conditions, the integration of the equations starts 12 months before we implement the fitting and study our model.

Fig. 3(a) shows the fit of our model to the data, where the abundance $M(t)$ is given as the number of female mosquitoes per night per trap. We observe that the mosquito population, which is assumed to be proportional to $M(t)$, increases in summer as expected. Although there are no daily abundance data to compare with, we remark that our model predicts day-to-day changes in the abundance of adult mosquitoes $M(t)$ due to fluctuations in temperature, humidity, and rainfall.

In Fig. 3(b) we plot the evolution of the immature population of mosquitoes $L(t)$ which shows that temperature and precipitation lead to more abrupt fluctuations in this group than in the compartment of adult mosquitoes. This was to be expected, since these climatic variables are directly introduced into the equation of the population of immature mosquitoes (see Eq. (1)). In turn,

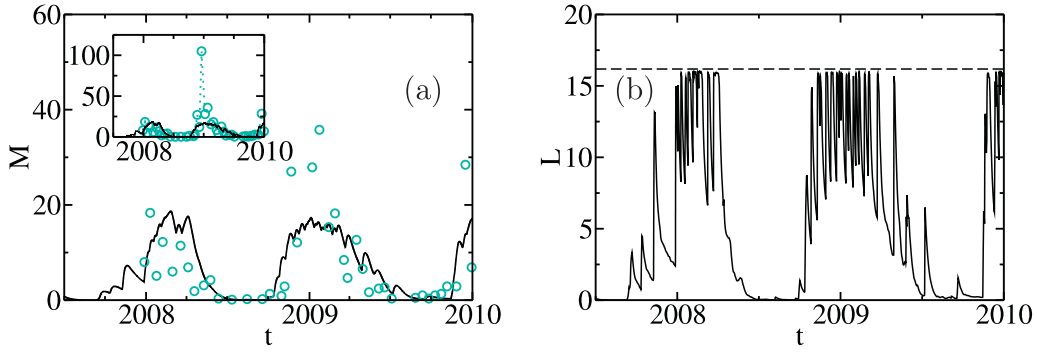

Fig. 3. Panel (a): Evolution of the abundance $M(t)$ of adult mosquitoes obtained from the fitted compartmental model. Large tick marks correspond to Jan 1. The blue circles represent the number of female mosquitoes collected in the city of Córdoba, and the black line corresponds to the model fit. Inset: main plot on a larger vertical scale showing an extremely high abundance data point. Panel (b): Evolution of the number of immature mosquitoes obtained from Eqs. (1)–(7). The dashed line represents the carrying capacity, K_L. (For interpretation of the references to color in this figure legend, the reader is referred to the web version of this article.)

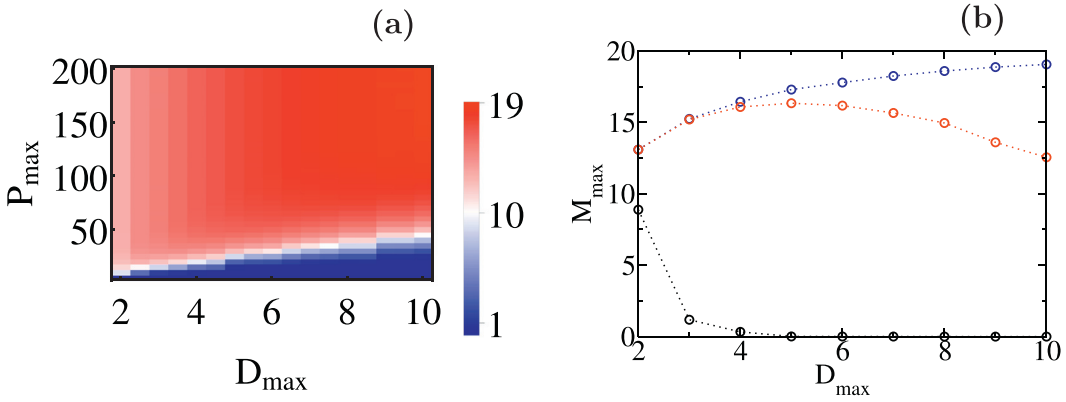

Fig. 4. Maximum number of mosquitoes M_{max} in the plane $P_{max} - D_{max}$ (a) and M_{max} as a function of D_{max} (b) for $P_{max} = 10$ mm (black), $P_{max} = 50$ mm (red) and $P_{max} = 190$ mm (blue). Dotted lines are to guide the eye. The results were obtained from Eqs. (1)–(7) and 10^4 stochastic realizations. (For interpretation of the references to color in this figure legend, the reader is referred to the web version of this article.)

we find that after a rainfall event, there is a large increase in the abundance of this group which frequently approaches the carrying capacity, leading to a subsequent population decline due to competition among immature mosquitoes (Roberts and Kokkinn, 2010; Suleman et al., 1982).

In the following section we study how different rainfall patterns affect the mosquito population dynamics.

3.2. *Effect of different rainfall regimes on* M_{max}

The proposed model of synthetic rainfall allows us to explore the evolution of mosquito abundance under possible scenarios in which the weather becomes, for instance, rainier, or with persistent drought conditions. In this Section we discuss how different rain regimes influence the mosquito population when it is at its highest (see Fig. 1(c)). To do this, we first assume that the total rainfall $P(m)$ (see Eq. (8)) is equally distributed in $D(m)$ days (see Eq. (9)), the remainder of the days in the month being rainless.

In Fig. 4(a) we consider the weather data of the austral summer season 2008–2009 (temperature and humidity), to show the influence of P_{max} and D_{max} on the highest peak M_{max} of mosquito abundance, with fixed values of the parameters $P_{min} = 10$ mm and $D_{min} = 1$.

From Fig. 4(a), we note that, for a fixed number of rainy days D_{max}, the highest peak of mosquito abundance increases as P_{max} grows since, as expected, a greater amount of water promotes breeding sites for mosquitoes. Similarly, it can be seen from Fig. 4(a) and (b) that for $P_{max} \approx 190$ mm, M_{max} is an increasing function with D_{max}, because a higher frequency of rainfall events provides more opportunities for mosquitoes to breed. The opposite happens for the lowest level of precipitation ($P_{max} \approx 10$ mm) as there is very little daily rainfall in this regime and the accumulated water evaporates quickly. Interestingly, we find that at moderate precipitation levels M_{max} has a maximum at an intermediate value of the number of rainy days. If the rainfall is equally distributed over a few days, the mosquito population will increase with more rainy days, but, beyond certain point, the rain becomes too thin to maintain all breeding sites active and the mosquito population must decrease. However, as it was mentioned above, the intensity of daily rainfalls is usually far from uniform (Wunderground, 2016), and recent studies suggest that the amount of mosquitoes depend on the distribution of precipitation (Bomblies, 2012; Bomblies et al., 2008; Cheng et al., 2016; Wang et al., 2016). Therefore, in the following we study how heterogeneity in the daily rainfall affects the dynamics of mosquito abundance.

In Fig. 5, using the weather data of the austral summer season 2008–2009 (temperature and humidity), we show the peak mosquito abundance for different values of P_{max}, D_{max}, and α, as obtained from the Eqs. (1)–(7). For simplicity, we use the same value of α for each month.

From Fig. 5(a), (b) and (d), we note that, similarly to the case of constant rainfall intensity, the abundance M_{max} is a decreasing (increasing) function with D_{max} for a low (high) amount of monthly precipitation P_{max}. Furthermore, Fig. 5(b)–(d) show that a higher variability in the intensity of rainfalls reduces the dependence of M_{max} with D_{max} with respect to the case of homogeneous rainfall. In particular, for $P_{max} = 10$ mm (see Fig. 5(b)), we note that M_{max} is higher in the heterogeneous case ($\alpha > 0$) than in the ho-

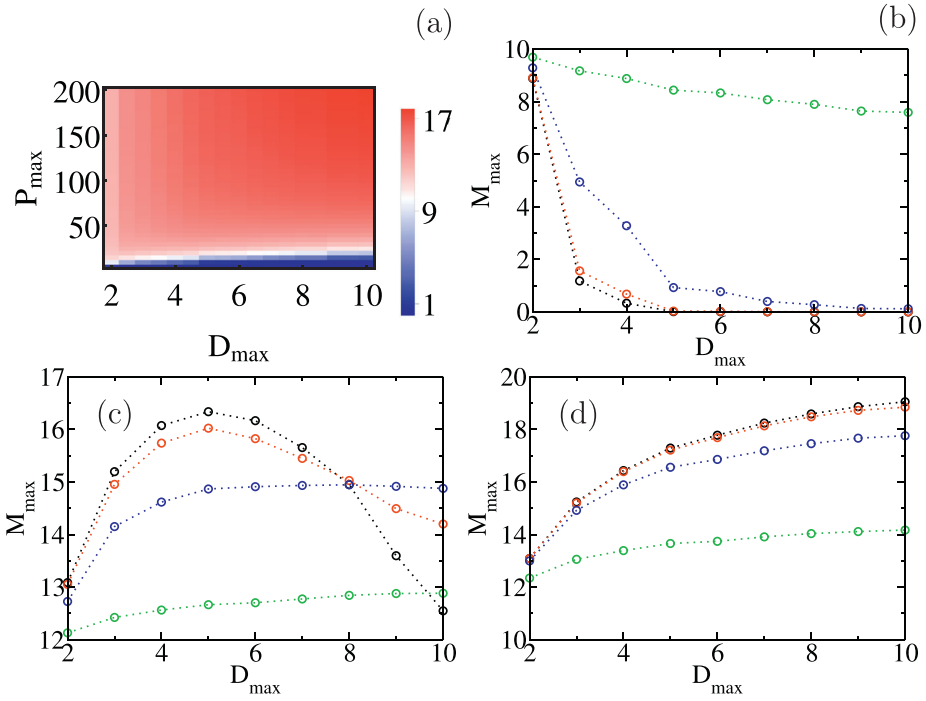

Fig. 5. Panel (a): Maximum number of mosquitoes M_{max} in the plane $P_{max} - D_{max}$ for $\alpha = 0.5$ and fixed values of the parameters $D_{min} = 1$ and $P_{min} = 10$ mm. Panel (b): M_{max} as a function of the number D_{max} of rainy days in the wettest month for $P_{max} = 10$ mm for different values of α. Rainy days have either the same amount of rainfall intensity (black), or $\alpha = 0.1$ (red), $\alpha = 0.5$ (blue), or $\alpha = 0.9$ (green). Panels (c) and (d) show the same as (b) for $P_{max} = 50$ mm and $P_{max} = 190$ mm, respectively. Averaging was made over 10^4 realizations of the rainfall time series $R(t)$. (For interpretation of the references to color in this figure legend, the reader is referred to the web version of this article.)

mogeneous one, since a greater variability tends to confine most of the total monthly precipitation to a few days, in which there is a higher level of water (see Eq. (6)) available for the immature mosquito population. In contrast, for $P_{max} = 190$ mm (see Fig. 5(d)) the heterogeneity diminishes the abundance M_{max} with respect to the homogeneous one. In this case, even if a higher amount of precipitation in a few days would increase the rate of immature mosquito birth, the effect of the intense rain days is limited by the threshold H_{max} because the impact of precipitation saturates for a precipitation higher than H_{max} (*i.e.*, $\lambda(t) = 1$, see Eqs. (6) and (7)). Moreover, there are more rainy days with low precipitation in this regime which further reduces the growth of mosquito population. As a consequence, the heterogeneity in the intensity of rainfall implies that the monthly total precipitation is a more relevant variable for the prediction of the maximum abundance of mosquitoes than the number of rainy days.

Another aspect of relevance for the prediction of vector-borne diseases is the effect of the rainfall in the dry-season (winter) on the future abundance of mosquitoes in summer. To study this relationship, we measure the maximum abundance of mosquitoes M_{max} and the timing τ_{max} at which the peak of mosquito abundance is reached (see Fig. 1(c)), for different values of P_{min} and D_{min}, which correspond to the parameters that control the intensity and frequency of rainfall in the driest month, respectively. Here, we keep fixed the parameters $P_{max} = 150$ mm and $D_{max} = 10$, and assume that February is always the wettest month of the year ($m_0 = 2$, see Eq. (8)). We note from Fig. 6(a) and (c) that, in the case of a homogeneous distribution of rainfalls, the time of peak τ_{max} moves forward for high values of P_{min} and D_{min}, because in this case the rainfalls are regular and abundant throughout the year, which favors mosquito breeding. However, for the explored values of P_{min} and D_{min}, the position of this peak is in late February or March, *i.e.*, just after the wettest month of the year. On the other hand, in a scenario of heterogeneous rainfalls with $\alpha = 0.9$ (see Fig. 6(b) and (d)), τ_{max} is moved forward by only approximately 10 days with respect to the homogeneous intensity case. Correspondingly, for constant values of α (0.1, 0.5 and 0.9) the changes in P_{min} and D_{min} only affect M_{max} by less than 5% (not shown here). Therefore these results suggest that the peak of abundance of mosquitoes and τ_{max} are mainly determined by summer weather conditions and the carrying capacity of the system and not by the intensity and distribution of precipitation throughout the year. Despite the weak effect of P_{min} on M_{max}, Fig. 6(e) and (f) show, as expected, that an increasing value of P_{min} could have a remarkable effect on the accumulated abundance of mosquitoes (one measure of which is the time integral of $M(t)$ over the period of interest), since from $P_{min} = 10$ mm to $P_{min} = 130$ mm, it could increase by more than 40%. However, for the case of a fixed value of P_{min} and higher values of α we obtain that the accumulated abundance of mosquitoes diminishes down to a 50% of the value for a homogeneous rain distribution. Consequently, the heterogeneity could help to attenuate the enhancement of the mosquito population. Therefore, these findings suggest that in order to predict the total annual abundance, it is not only necessary to take into account the overall amount of rainfall throughout the year but also the heterogeneity in daily rainfall intensity.

4. Discussion

Since projections of climate change (Nuñez et al., 2009) suggest that for the late twenty-first century in regions of South America, such as Córdoba province, the pattern of precipitation will change towards a regime with rainier autumns and an increase in the extreme events, it is crucial to study how this variation would affect the mosquito abundance.

In this paper we studied the effects of the total intensity, number of rainy days and heterogeneity of rainfall on the mosquito population. We found that for a regime with a low total rainfall,

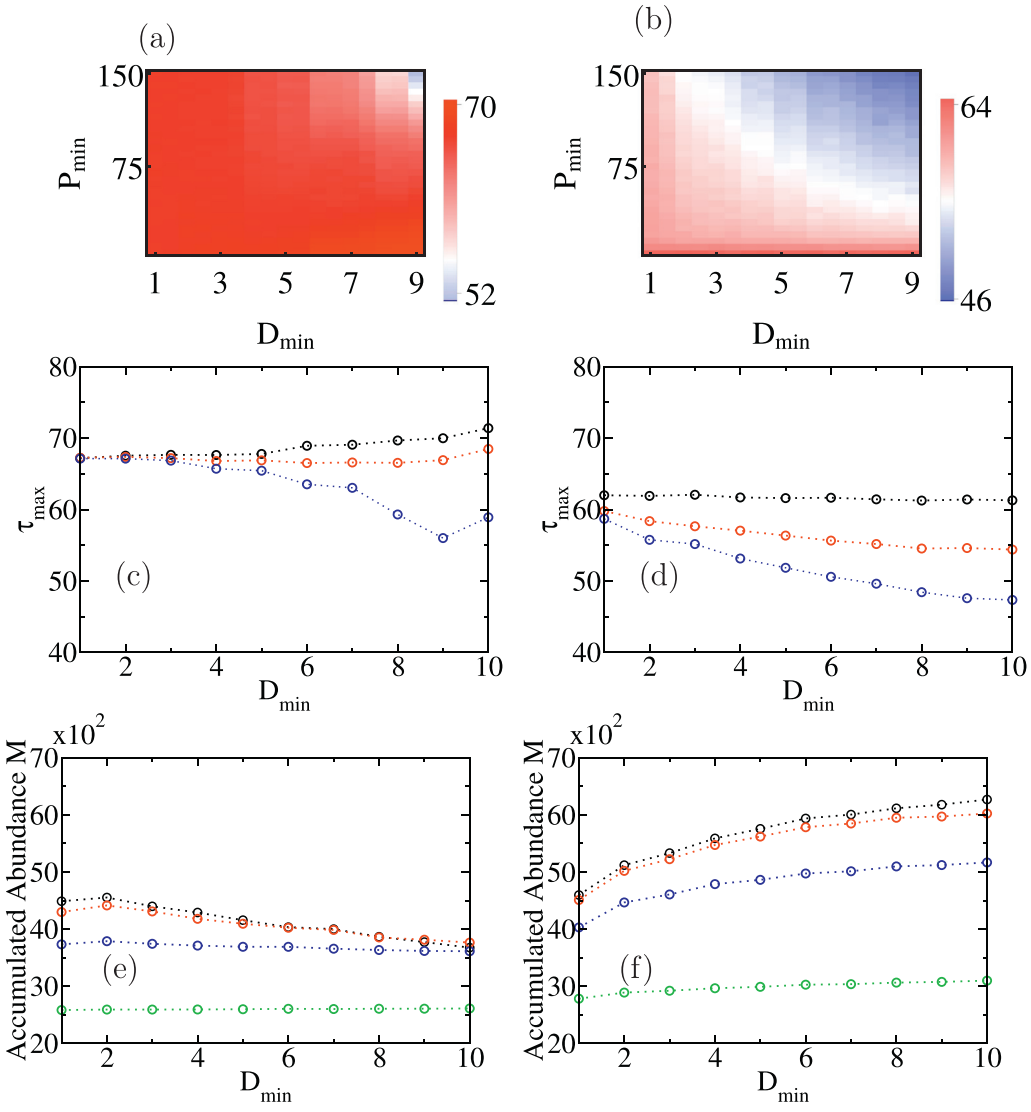

Fig. 6. Panels (a) and (b): Time τ_{max} (measured in days, where $\tau_{max} = 0$ corresponds to January 1, 2009) at which the peak of mosquito abundance is reached in the plane $P_{min} - D_{min}$ for a homogeneous intensity distribution of rainfalls (a) and $\alpha = 0.9$ (b). Panels (c) and (d): τ_{max} as a function of the number of rainy days in the driest month, D_{min}, for a homogeneous intensity distribution of rainfalls (c) and $\alpha = 0.9$ (d) for various values of P_{min}: 10 mm (black), 50 mm (red) and 130 mm (blue). Panels (e) and (f): accumulated mosquito abundance between July 2008 and July 2009 as a function of D_{min}, with $P_{min} = 10$ mm (e) and $P_{min} = 130$ mm (f) for: homogeneous rainfall intensity (black), $\alpha = 0.1$ (red), $\alpha = 0.5$ (blue) and $\alpha = 0.9$ (green). The dotted lines are a guide to the eye. The figures were obtained averaging over 10^5 realizations of the rainfall time series $R(t)$. (For interpretation of the references to color in this figure legend, the reader is referred to the web version of this article.)

the abundance of mosquitoes is a decreasing function with the number of rainy days, while for a high total rainfall regime it is an increasing function of this number. Interestingly, for an intermediate precipitation regime, we found that there is a halfway number D_{max} of rainy days for which M_{max} is optimized. Since P_{max} is fixed, fewer rainy days would imply dry intervals, leading to a lessening of the mosquito abundance. If the number of rainy days exceeds the optimal value of D_{max}, a considerable fraction of the rainwater resulting from the typically meager rainfall would disappear due to evapotranspiration, again leading to a reduction of the mosquito abundance.

In order to study the effect of the heterogeneity in the daily rainfall, we used a fracturing process that keeps constant the total amount of monthly precipitation. We observed that a higher heterogeneity reduces the dependence of M_{max} on the number of rainy days. However, an increasing variability favors the mosquito production in the low rainfall regime, while the opposite behavior takes place in the case of high precipitation P_{max}. Therefore, if climatic models predict the intensification of storms, but not an increase in the total amount of precipitation, our model predicts that the enhancement of mosquito abundance would be more significant in semiarid areas than in humid climates.

Finally we study the effect of an increasing amount of rainfall in the dry season on the mosquito abundance dynamics, obtaining that high precipitation throughout the year does not significantly alter the maximum abundance or the time at which this peak occurs, but it could notably increase the accumulated abundance of mosquitoes. However, we also observed that a regime with a higher variability of rainfall intensity could reduce this increase.

While our model captures multiple relationships between rainfall and mosquito population, additional extensions could be considered. For instance, there is evidence that rainfalls reduce the immature population in the short term due to flushing of breeding sites (Gardner et al., 2012; Strickman, 1988) and affect the bacterial concentration used as food by mosquito larvae (Chaves and Kitron, 2011); therefore, it would be interesting to study the relevance of these effects on the dynamic of mosquito population.

We think that our findings could be used as support and reference guidance for the assessment of the influence of different rainfall regimes on the mosquito population dynamics, using the weather data for any specific region. Such an assessment would impact positively on our ability to make predictions for the spread of various possible arboviruses. It is also known that rainfall could have a substantial effect on insecticide residence times (Allan et al., 2009). The model presented here can be used to optimize the efficacy of mosquito control campaigns, using temperature and rainfall data to select the best times for the application of population reduction procedures.

Acknowledgments

This work was supported by SECyT-UNC (Projects 103/15 and 313/16), CONICET (PIP 11220110100794), and PICT Cambio Climático (Ministerio de Ciencia y Técnica de la Provincia de Córdoba), PICT Nro. 2013-1779 (ANPCYT-MYNCYT), Argentina. We also thank Dr. A. M. Visintin and Biól. M. Beranek for useful discussions.

Appendix A. Calibration

The Metropolis-Hastings (MH) algorithm is a stochastic optimization tool for fitting statistical models to data that has been used in cosmology (Christensen et al., 2001; 2004; Lewis and Bridle, 2002), epidemiology (Merler et al., 2015), and in the study of mosquito population dynamics (Marini et al., 2016). This algorithm allows us to estimate the unknown values of some parameters Θ (Θ represents either a single parameter or a parameter set), by means of a stochastic search in the parameter space that generates a sequence or chain $\Theta^{(i)}$, where i represents the step number of the MH algorithm (Bonamente, 2013). Each value of this chain is sampled from a proposal distribution and accepted with a probability σ defined by an acceptance function, which depends on the likelihood function of the observations.

In our model we estimate the parameters β_L, H_{max}, H_{min} and K_L using a MH algorithm and the data for adult mosquito abundance from Córdoba city in the period 2008–2009 (Batallán, 2013; Batallán et al., 2015). We propose that the likelihood of the observations is given by

$$L = \prod_{j=1}^{n} p(x_j(H_{max}, H_{min}, K_L, \beta_L); k_j), \tag{A.1}$$

where n is the number of data points and $p(x_j(H_{max}, H_{min}, K_L, \beta_L); k_j)$ is the probability to observe the abundance k_j of mosquitoes obtained from the data. Here we assume that $p(\cdot)$ follows a Poisson distribution whose mean $x(H_{max}, H_{min}, K_L, \beta_L)$ is the number of adult mosquitoes predicted by Eqs. (1)–(7).

The MH algorithm implemented in this paper has the following steps:

- Step 1: Initialize the starting value of the parameters $\Theta^{(i=0)}$, using a uniform distribution in order to avoid favoring any initial value.
- Step 2: Generate a new sample of the parameters, Θ^{New} starting from a proposal distribution that indicates a candidate for the next sample value. To ensure that the new values of the parameters are positive, we use as a proposal distribution a log-normal density which has a mean equal to the logarithm of the current value parameter and constant variance δ. The value of this variance is chosen in order to guarantee an acceptance rate between 10% and 30% in the burn-in period.
- Step 3: accept the new candidate Θ^{New} with probability σ:

$$\sigma = min\left\{1, \frac{L(\Theta^{New})}{L(\Theta^{(i)})}\right\}. \tag{A.2}$$

- Step 4: repeat steps 2 and 3 until convergence is reached.

We perform 2.10^6 iterations and check convergence by visual inspection of the chain $\Theta^{(i)}$. In order to construct the posterior distribution of the parameters, we discard the first 10^5 iterations as a

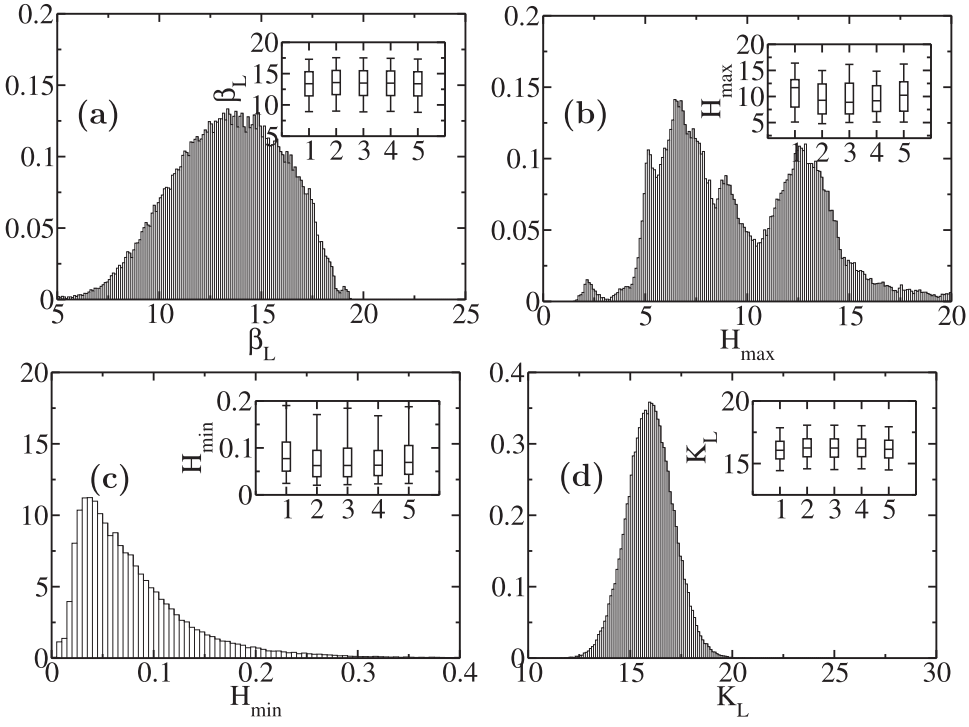

Fig. A.1. Posterior distribution obtained in the steady state of the MH algorithm from 2.10^6 iterations, using 10^5 iterations as a burn in for the parameters β_L (a), H_{max} (b), H_{min} (c), and K_L (d). In the insets we show the boxplot obtained from the posterior distribution in the steady state for 5 different initial conditions (see step one of the MH algorithm).

burn-in and we only keep every 20th sampled value of the remaining iterations to reduce autocorrelation within successive samples. Finally, the values of the parameters that we will use in our model are the averages of the medians of the posterior distributions obtained from 5 different initial conditions (see step one of the MH algorithm).

Fig. A.1 shows the posterior distribution obtained for the parameters β_L, H_{max}, H_{min} and K_L. We note that all of these distributions are unimodal, except for H_{max}. Although in this paper we set $H_{max} = 9.86$ mm, since it is the average value of the median obtained from the MH algorithm, we also check our model for $H_{max} \approx 7$ mm and $H_{max} \approx 13$ mm which are the positions of the highest peaks of the posterior distribution (see Fig. A.1(b)). For these cases, our results presented in Section 3 do no qualitatively change.

Appendix B. Fracturing process

Fracturing process (FT) is a stochastic iterative process which generates a finite sequence of numbers with the property that their sum is always a constant (Borgos, 2000; Finley and Kilkki, 2014). From a geometrical point of view, this method consists of partitioning an interval of length ℓ in a number D of subintervals or segments, with the property that the sum of their lengths is always ℓ. Following Finley and Kilkki (2014), the FT process starts with an interval or segment of length ℓ which is split into two subintervals of lengths $\tilde{\ell}$ and $\ell - \tilde{\ell}$, where $\tilde{\ell}$ is a stochastic variable generated by the following function:

$$\tilde{\ell} = \ell \times \begin{cases} \rho \dfrac{1-\alpha}{\alpha} & \text{if } 0 \le \rho < \dfrac{\alpha}{2} \\ \dfrac{1}{2} + \left(\rho - \dfrac{1}{2}\right)\dfrac{\alpha}{1-\alpha} & \text{if } \dfrac{\alpha}{2} \le \rho \le 1 - \dfrac{\alpha}{2} \\ 1 - (1-\rho)\dfrac{1-\alpha}{\alpha} & \text{if } 1 - \dfrac{\alpha}{2} < \rho \le 1 \end{cases} \tag{B.1}$$

Here ρ is a uniform random variable and $\alpha \in (0, 1)$ is a parameter that controls the average length $\tilde{\ell}$. In a second step, the partition function, Eq. (B.1), is applied again on the intervals resulting from the previous step, generating a total of 4 intervals. This procedure is repeated until the required number of intervals is reached[1].

In order to model the variability in the daily rainfall $R(t)$, we apply a FT process for each month, in which,

- the length of the initial segment ℓ is given by Eq. (8), *i.e.*, the monthly precipitation,
- the number D of subintervals is given by Eq. (9), *i.e.*, the number of rainy days.

After we apply the fracturing process, the length of each resulting interval $\tilde{\ell}_i$ (with $i = 1, \cdots, D$) represents the total amount of water that falls in the day d_i, which we choose at random as it is shown in the schematic of Fig. B.1, and then we set $R(d_i) = \tilde{\ell}_i$.

In Fig. B.2 we plot the distribution of segment lengths obtained from an FT process for $\ell = 150$ mm and $D = 10$, which are the average rainfall and the number of rainy days in February, respectively. Here we use the value of $\alpha = 0.43$ which gives the best fit to the February rainfalls in the city of Córdoba in the period 2001–2015.

Appendix C. Sensitivity analysis

A sensitivity analysis allows us to measure the impact of different parameters on the relevant variables of our model. In this section, we perform a one-way sensitivity analysis on the model of Section 2.1, by varying a ± 25% of the baseline values of individual parameters one at a time, while keeping the other parameters constant in order to analyze their individual impact on the maximum abundance of mosquitoes M_{max}. The parameters examined are: β_L, H_{max}, H_{min}, and K_L. The results of the sensitivity analysis are summarized in Table C.1.

It shows, as expected, that for higher values of β_L, H_{max}, H_{min}, and K_L the abundance M_{max} increases. Although the influence of the first three is rather weak, M_{max} is heavily influenced by K_L, which is therefore a critical parameter for the estimation of mosquito abundance.

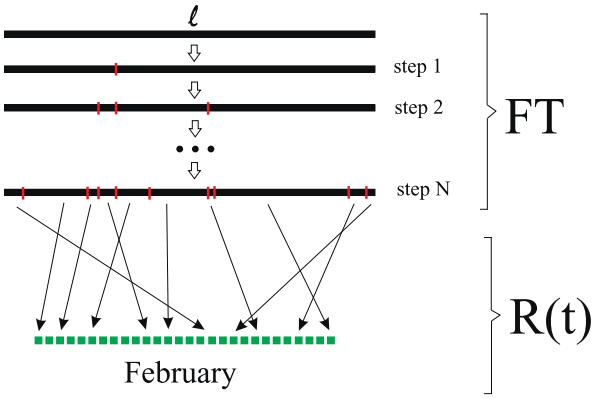

Fig. B.1. Schematic of the construction of $R(t)$ corresponding to February. At the top of the figure we show the FT process and at the bottom the construction of $R(t)$, in which each square represents a day in February. The FT process stops when the required number of subintervals (given by Eq. (9)) is reached. The length of each of these segments represents the rainfall in one day in February, which is randomly chosen. Those days that are not associated with any length of the FT process, have $R(t) = 0$.

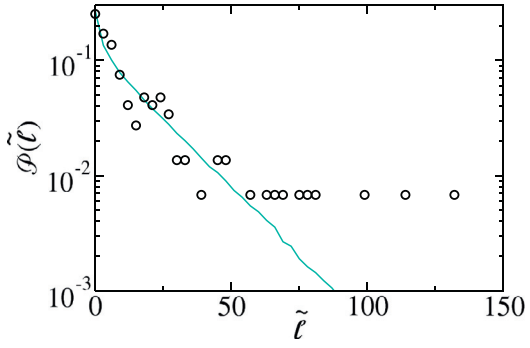

Fig. B.2. Observed February rainfall distribution in Córdoba during the period 2001–2015 (symbols) and distribution of segment lengths $\mathcal{P}(\tilde{\ell})$ for $\ell = 150$ mm, and $D = 10$, and $\alpha = 0.43$ (solid line) obtained over 2.10^4 realizations.

Table C.1
Variation of the maximum abundance of mosquitoes ($M_{max} = 17.3$) when it is applied a one-way sensitivity analysis.

Parameter	−25%	+25%
β_L	−2.1%	+1%
H_{max}	−0.4%	+0.9%
H_{min}	−0.7%	+0.6%
K_L	−25%	+25%

[1] For example, in order to generate a total of five subintervals, three iterations of the fracturing process must be performed: step 1) the initial interval is divided into two subintervals, step 2) each of the previous subintervals is divided into two parts, and finally step 3) one randomly chosen subinterval of the previous step is split into two subintervals.

References

Allan, S.A., Kline, D.L., Walker, T., 2009. Environmental factors affecting efficacy of bifenthrin-treated vegetation for mosquito control. J. Am. Mosq. Control Assoc. 25 (3), 338–346. doi:10.2987/09-5854.1.

Almirón, W.R., Brewer, M.E., 1996. Winter biology of Culex pipiens quinquefasciatus say,(diptera: Culicidae) from Córdoba, Argentina. Mem. Inst. Oswaldo Cruz 91, 649–654. doi:10.1590/S0074-02761996000500019.

Anderson, R.M., May, R.M., Anderson, B., 1992. Infectious Diseases of Humans: Dynamics and Control, vol. 28. Wiley Online Library.

Batallán, G.P., 2013. Bionomía de Culex interfor Dyar en Córdoba, Argentina. Facultad de Ciencias Exactas Físicas y Naturales, Universidad Nacional de Córdoba PhD thesis.

Batallán, G.P., Estallo, E.L., Flores, F.S., Sartor, P., Contigiani, M.S., Almirón, W.R., 2015. St. Louis Encephalitis virus mosquito vectors dynamics in three different environments in relation to remotely sensed environmental conditions. Acta Trop. 146, 53–59. doi:10.1016/j.actatropica.2015.03.009.

Beltrán, F.J., Díaz, L.A., Konigheim, B., Molina, J., Beaudoin, J.B., Contigiani, M., Spinsanti, L.I., 2015. Evidencia serológica de circulación del virus de la encefalitis de San Luis en aves de la Ciudad Autónoma de Buenos Aires, Argentina. Rev. Argent. Microbiol. 47, 312–316. doi:10.1016/j.ram.2015.09.002.

Bomblies, A., 2012. Modeling the role of rainfall patterns in seasonal malaria transmission. Clim. Change 112 (3–4), 673–685. doi:10.1007/s10584-011-0230-6.

Bomblies, A., Duchemin, J.-B., Eltahir, E.A.B., 2008. Hydrology of malaria: model development and application to a Sahelian village. Water Resour. Res. 44 (12). doi:10.1029/2008WR006917.

Bonamente, M., 2013. Statistics and Analysis of Scientific Data. Springer.

Borgos, H.G., 2000. Partitioning of a line segment. Stochastic Modeling and Statistical Inference of Geological Fault Populations and Patterns. Norwegian University of Science and Technology.

Chaves, L.F., Kitron, U.D., 2011. Weather variability impacts on oviposition dynamics of the southern house mosquito at intermediate time scales. Bull. Entomol. Res. 101, 633–641. doi:10.1017/S0007485310000519.

Cheng, Q., Jing, Q., Spear, R.C., Marshall, J.M., Yang, Z., Gong, P., 2016. Climate and the timing of imported cases as determinants of the dengue outbreak in Guangzhou, 2014: evidence from a mathematical model. PLoS Negl. Trop. Dis. 10, e0004417. doi:10.1371/journal.pntd.0004417.

Cho, H.-K., Bowman, K.P., North, G.R., 2004. A comparison of gamma and lognormal distributions for characterizing satellite rain rates from the tropical rainfall measuring mission. J. Appl. Meteorol. 43, 1586–1597. doi:10.1175/JAM2165.1.

Christensen, N., Meyer, R., Knox, L., Luey, B., 2001. Bayesian methods for cosmological parameter estimation from cosmic microwave background measurements. Class. Quantum Grav. 18, 2677. doi:10.1088/0264-9381/18/14/306.

Christensen, N., Meyer, R., Libson, A., 2004. A Metropolis–Hastings routine for estimating parameters from compact binary inspiral events with laser interferometric gravitational radiation data. Class. Quantum Grav. 21, 317. doi:10.1088/0264-9381/21/1/023.

Ciota, A.T., Matacchiero, A.C., Kilpatrick, A.M., Kramer, L.D., 2014. The effect of temperature on life history traits of Culex mosquitoes. J. Med. Entomol. 51, 55–62. doi:10.1603/ME13003.

David, M.R., Ribeiro, G.S., Maciel-de-Freitas, R., 2012. Bionomics of Culex quinquefasciatus within urban areas of Rio de Janeiro, Southeastern Brazil. Rev. Saúde Pública 46, 858–865. doi:10.1590/S0034-89102012000500013.

Deidda, R., 2010. A multiple threshold method for fitting the generalized Pareto distribution to rainfall time series. Hydrol. Earth. Syst. Sci. 14, 2559–2575. doi:10.5194/hess-14-2559-2010.

Diaz, L.A., Flores, F.S., Beranek, M., Rivarola, M.E., Almirón, W.R., Contigiani, M.S., 2013. Transmission of endemic St Louis encephalitis virus strains by local Culex quinquefasciatus populations in Córdoba, Argentina. Trans. R. Soc. Trop. Med. Hyg. 107 (5), 332–334. doi:10.1093/trstmh/trt023.

Diaz, L.A., Occelli, M., Ludueña-Almeida, F., Almiron, W.R., Contigiani, M.S., 2008. Eared dove (Zenaida Auriculata, Columbidae) as host for St. Louis encephalitis virus (Flaviviridae, Flavivirus). Vector Borne Zoonotic Dis. 8, 277–282. doi:10.1089/vbz.2007.0168.

Diaz, L.A., Quaglia, A.I., Konigheim, B.S., Boris, A.S., Aguilar, J.J., Komar, N., Contigiani, M.S., 2016. Activity patterns of St. Louis encephalitis and West Nile viruses in free ranging birds during a human encephalitis outbreak in Argentina. PLoS One 11, e0161871. doi:10.1371/journal.pone.0161871.

Ewing, D.A., Cobbold, C.A., Purse, B.V., Nunn, M.A., White, S.M., 2016. Modelling the effect of temperature on the seasonal population dynamics of temperate mosquitoes. J. Theor. Biol. 400, 65–79. doi:10.1016/j.jtbi.2016.04.008.

Finley, B.J., Kilkki, K., 2014. Exploring empirical rank-frequency distributions longitudinally through a simple stochastic process. PLoS One 9, e94920. doi:10.1371/journal.pone.0094920.

Gardner, A.M., Hamer, G.L., Hines, A.M., Newman, C.M., Walker, E.D., Ruiz, M.O., 2012. Weather variability affects abundance of larval Culex (Diptera: Culicidae) in storm water catch basins in suburban Chicago. J. Med. Entomol. 49, 270–276. doi:10.1603/ME11073.

Gong, H., DeGaetano, A.T., Harrington, L.C., 2011. Climate-based models for west nile culex mosquito vectors in the northeastern us. Int. J. Biometeorol. 55 (3), 435–446. 10.1007/s00484-010-0354-9

Gubler, D.J., 2002. The global emergence/resurgence of arboviral diseases as public health problems. Arch. Med. Res. 33, 330–342. doi:10.1016/S0188-4409(02)00378-8.

Gubler, D.J., Kuno, G., Markoff, L., et al., 2007. Flaviviruses. In: Fields, B.N., Knipe, D.M., Howley, P.M. (Eds.), Fields Virology. Lippincott Williams & Wilkins, pp. 1153–1253.

Gunay, F., Alten, B., Ozsoy, E.D., 2011. Narrow-sense heritability of body size and its response to different developmental temperatures in Culex quinquefasciatus (Say 1923). J. Vector Ecol. 36, 348–354. doi:10.1111/j.1948-7134.2011.00175.x.

Harrigan, R.J., Thomassen, H.A., Buermann, W., Smith, T.B., 2014. A continental risk assessment of West Nile virus under climate change. Glob. Change Biol. 20, 2417–2425. doi:10.1111/gcb.12534.

Hernandez, G., 2003. Two-dimensional model for binary fragmentation process with random system of forces, random stopping and material resistance. Physica A 323, 1–8. doi:10.1016/S0378-4371(03)00032-3.

Jarsún, B., Gorgas, J.A., Zamora, E., Bosnero, E., Lovera, E., Ravelo, A., Tassile, J.L., 2003. Caracterización general de la provincia. In: Gorgas, J.A., Tassile, J.L. (Eds.), Recursos Naturales de la Provincia de Córdoba, Los Suelos. Agencia Córdoba Ambiente e INTA, Córdoba, pp. 23–60.

Karl, S., Halder, N., Kelso, J.K., Ritchie, S.A., Milne, G.J., 2014. A spatial simulation model for dengue virus infection in urban areas. BMC Infect. Dis. 14, 1. doi:10.1186/1471-2334-14-447.

Kilpatrick, A.M., 2011. Globalization, land use, and the invasion of West Nile virus. Science 334, 323–327. doi:10.1126/science.1201010.

Lei, M., Niyogi, D., Kishtawal, C., Pielke Sr, R., BeltrÃąn-Przekurat, A., Nobis, T., Vaidya, S., 2008. Effect of explicit urban land surface representation on the simulation of the 26 july 2005 heavy rain event over mumbai, india. Atmos. Chem. Phys. 8 (20), 5975–5995. doi:10.5194/acp-8-5975-2008.

Lewis, A., Bridle, S., 2002. Cosmological parameters from CMB and other data: a Monte Carlo approach. Phys. Rev. D 66, 103511. doi:10.1103/PhysRevD.66.103511.

Li, X., Zhang, Q., Ye, X., 2013. Dry/wet conditions monitoring based on trmm rainfall data and its reliability validation over poyang lake basin, china. Water 5 (4), 1848–1864. doi:10.3390/w5041848.

Loetti, V., Schweigmann, N., Burroni, N., 2011. Development rates, larval survivorship and wing length of Culex pipiens (Diptera: Culicidae) at constant temperatures. J. Nat. Hist. 45, 2207–2217. doi:10.1080/00222933.2011.590946.

Lord, C.C., Day, J.F., 2001a. Simulation studies of St. Louis encephalitis and West Nile viruses: the impact of bird mortality. Vector-Borne Zoonotic Dis. 1, 317–329. doi:10.1089/15303660160025930.

Lord, C.C., Day, J.F., 2001b. Simulation studies of St. Louis encephalitis virus in South Florida. Vector-Borne Zoonotic Dis. 1, 299–315. doi:10.1089/15303660160025921.

Lumsden, L., 1958. St. Louis encephalitis in 1933: observations on epidemiological features. Public Health Rep. 73 (4), 340.

Madsen, H., Arnbjerg-Nielsen, K., Mikkelsen, P.S., 2009. Update of regional intensity–duration–frequency curves in Denmark: tendency towards increased storm intensities. Atmos. Res. 92, 343–349. doi:10.1016/j.atmosres.2009.01.013.

Marini, G., Poletti, P., Giacobini, M., Pugliese, A., Merler, S., Rosà, R., 2016. The role of climatic and density dependent factors in shaping mosquito population dynamics: the case of Culex pipiens in Northwestern Italy. PLoS One 11, e0154018. doi:10.1371/journal.pone.0154018.

Merler, S., Ajelli, M., Fumanelli, L., Gomes, M.F., Pastore y Piontti, A., Rossi, L., Chao, D.L., Longini, I.M., Halloran, M.E., Vespignani, A., 2015. Spatiotemporal spread of the 2014 outbreak of Ebola virus disease in Liberia and the effectiveness of non-pharmaceutical interventions: a computational modelling analysis. Lancet. Infect. Dis. 15, 204–211. doi:10.1016/S1473-3099(14)71074-6.

Nelms, B.M., Macedo, P.A., Kothera, L., Savage, H.M., Reisen, W.K., 2013. Overwintering biology of Culex (Diptera: Culicidae) mosquitoes in the Sacramento Valley of California. J. Med. Entomol. 50, 773–790. doi:10.1603/ME12280.

Nuñez, M.N., Solman, S.A., Cabré, M.F., 2009. Regional climate change experiments over southern South America. II: climate change scenarios in the late twenty-first century. Clim. Dyn. 32, 1081–1095. doi:10.1007/s00382-008-0449-8.

Oda, T., Mori, A., Ueda, M., Kurokawa, K., et al., 1980. Effects of temperatures on the oviposition and hatching of eggs in culex pipiens molestus and culex pipiens quinquefasciatus. Trop. Med. 22 (3), 167–180.

Olson, J.G., Atmosoedjono, S., Lee, V.H., Ksiazek, T.G., 1983. Correlation between population indices of Culex Tritaeniorhynchus and Cx. Gelidus (Diptera: Culicidae) and rainfall in Kapuk, Indonesia. J. Med. Entomol. 20, 108–109. doi:10.1093/jmedent/20.1.108.

Owusu, K., Waylen, P.R., 2013. The changing rainy season climatology of mid-Ghana. Theor. Appl. Climatol. 112, 419–430. doi:10.1007/s00704-012-0736-5.

Reisen, W.K., Cayan, D., Tyree, M., Barker, C.M., Eldridge, B., Dettinger, M., 2008. Impact of climate variation on mosquito abundance in California. J. Vector Ecol. 33, 89–98. doi:10.3376/1081-1710(2008)33[89:IOCVOM]2.0.CO;2.

Ribeiro, P.B., Costa, P.R., Loeck, A.E., Vianna, É.E., Silveira Júnior, P., 2004. Thermal requeriments of Culex quinquefasciatus (Diptera, Culicidae) in Pelotas, Rio Grande do Sul, Brazil. Iheringia. Série Zoologia 94 (2), 177–180. doi:10.1590/S0073-47212004000200010.

Roberts, D., Kokkinn, M., 2010. Larval crowding effects on the mosquito Culex quinquefasciatus: physical or chemical? Entomol. Exp. Appl. 135 (3), 271–275. doi:10.1111/j.1570-7458.2010.00993.x.

Romanenko, V., 1961. Computation of the autumn soil moisture using a universal relationship for a large area. In: Proceedings Ukrainian Hydrometeorological Research Institute (Kiev), p. 3.

Strickman, D., 1988. Rate of oviposition by Culex quinquefasciatus in San Antonio, Texas, during three years. J. Am. Mosq. Control Assoc. 3, 339–344.

Suhaila, J., Jemain, A.A., 2007. Fitting daily rainfall amount in Malaysia using the normal transform distribution. J. Appl. Sci. 7, 1880–1886. doi:10.3923/jas.2007.1880.1886.

Suleman, M., et al., 1982. The effects of intraspecific competition for food and space on the larval development of Culex quinquefasciatus. Mosq. News 42 (3), 347–356.

Valipour, M., 2014. Application of new mass transfer formulae for computation of evapotranspiration. J. Appl. Water Eng. Res. 2, 33–46. doi:10.1080/23249676.2014.923790.

Wang, X., Tang, S., Cheke, R.A., 2016. A stage structured mosquito model incorporating effects of precipitation and daily temperature fluctuations. J. Theor. Biol. 411, 27–36. doi:10.1016/j.jtbi.2016.09.015.

Wunderground, 2016. http://www.wunderground.com (Accessed: 25th April 2016).

Zhai, P., Zhang, X., Wan, H., Pan, X., 2005. Trends in total precipitation and frequency of daily precipitation extremes over China. J. Climate 18, 1096–1108. doi:10.1175/JCLI-3318.1.